

Electromagnetic Soil Moisture Sensor (ESMS)

Final Report

Kyle Richard, Nicholas Keith, Erik Sprague, Mohamed A. Mohamed

Abstract – Electromagnetic Soil Moisture Sensor is an electromagnetic system that allow users to map moisture levels over a small area of soil. It detects the power of the electromagnetic energy radiated from the soil using an antenna. Soil moisture is a key variable in controlling water and heat energy between the land surface and the atmosphere. Therefore, soil moisture plays an important role in the development of weather patterns. The signal captured is then fed into a Radio Frequency (RF) receiver, where it's amplified and filtered. The filtered data is then saved on a micro SD card. The data in the SD card is processed in a computer to produce a position vs. brightness temperature map of the landscape.

Index Terms – Radiometry, Emissivity, Brightness Temperature

I. INTRODUCTION

SUSTAINABILITY is a social movement that aims to create a human lifestyle that preserves the earth's natural resources. We now live in a modern, consumerist, and largely urban existence throughout the developed world, where we consume a lot of natural resources every day. One of these largely consumed resources is water. One of the most urgent challenges facing our world today is ensuring an adequate supply and quality of water in light of our increased need and climate change. The agricultural sector consumes about 70% of the planet's accessible freshwater – more than twice that of industry (23%), and municipal use (8%) [8]. ESMS will help farmers reduce water waste significantly, by allowing farmers to distribute water efficiently across their landscapes.

A. Current Solutions

The most effective current solutions involve radiometers or radar systems [1]. The premise of this is that water in soil decreases the soil's emissivity. Power radiated is proportional to brightness temperature: $P=KT_B B$, where K is Boltzmann's constant, T_B is brightness temperature and B is bandwidth. $T_B = e*T$, where e is emissivity and T is the true temperature. Soil of the same temperature with different water content will radiate different power levels. By directing an antenna at a certain area and measuring the power received, the brightness temperature of that area can

be determined. This is also known as the “antenna temperature.”

NASA developed such a system. They launched the Soil Moisture Active Passive (SMAP) mission on January 31, 2015 [2]. The SMAP system consists of a radar and a radiometer system that penetrates into the top 2 inches of the soil. This mission will improve climate and weather forecasts and allow scientists to monitor droughts and predict floods and storms earlier and better. However, it was built on large scale to see moisture levels across continents using satellites.

Handheld moisture sensors have also been built that require their user to place a pin into the soil to get a moisture reading, but this method is both tiresome and time-consuming. It is mainly used in construction to check moisture levels under construction sites. These tools are not always accurate and are not very efficient for farms.

B. Our Solution

To make radiometer technology more available to users on a small scale, we would like to make a radiometer system that could be mounted on a tractor or a drone. The ideal case would be a drone-mounted system, but we will prioritize the radiometric aspect and mount it to a drone if time permits.

With our project, a small-scale farmer could be able to map out the moisture in his or her fields. Using this information, the farmer can optimize their irrigation system and save water. During a time where water is becoming more scarce, especially in the western part of the country, this could mitigate the necessity for limitations on water use in areas experiencing drought.

Additionally, our project could be used by companies hoping to do construction on previously untouched lands. The ESMS may be used to quickly determine whether the land of interest is a wetland, which would save time and money for the owner of the land and the construction company.

C. Specifications

Figure 1 lists the specifications for ESMS. The specifications include operation time, system weight, and measurement precision. We anticipate that our system will be drawing 352 mA from a 11.1 V battery. The battery has a capacity of 22mA hours, therefore our system could operate for 6 hours. The reason for having an operation time of 30 minutes is that in the ideal case that the system is mounted to a drone, the drone would likely not be able to fly with a large payload for more than 30 minutes. The heavier the payload of a drone, the shorter the flight time. This leads into the overall system weight specification, we want to build a system that is less than 3kg. After researching we discovered there are drones that have the ability to fly for 30 min while carrying this payload. The last specification is radiometric sensitivity of less than 1 kelvin. Meaning our radiometer would be able to measure brightness temperature to the accuracy of 1 kelvin. Brightness temperature is proportional to the percentage of water in the soil. A study done at Purdue University, called Soil Moisture Sensing with Microwave Radiometers, researched the connection between soil moisture and brightness temperature. In the experiment they measured a bare field with a relatively smooth surface. For comparison purposes they measure this field at wet and dry conditions. There was about a 70k difference for a 14 % difference in the soil moisture. Meaning every 1% change in water concentration is equivalent to a brightness temperature change of 5K.

System Requirements	Specs
Operation Time	30 min
System Overall Weight	< 3kg
Measurement Precision	$\Delta T < 5$ Kelvin

Figure 1. ESMS System Requirements

II. DESIGN

Figure 2 shows our system block diagram. The major components comprising our project are an RF receiver, a control circuit, various sensors to collect data, and a power supply. The RF receiver consists of an antenna, a circuit to amplify and filter the antenna signal, and a power detector which produces a DC output voltage from which the received signal's input power may be determined. This voltage will be sampled by our microcontroller along with readings from two reference sources. The data will be stored in an SD card and placed into a computer program after collection. The program will utilize the power readings from the antenna and two reference sources to determine the antenna temperature. Soil with a high moisture content will

cause a lower antenna temperature, and that with a low moisture content will cause a higher reading.

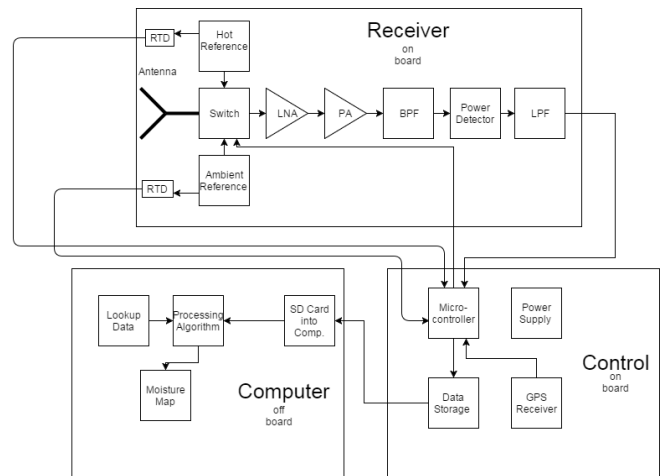


Figure 2. System Block Diagram

1. RF Antenna and Receiver

For the antenna, we acquired a microstrip-patch antenna from the MIRSL (Microwave Instructional Remote Sensing Laboratory). Designing a microstrip patch antenna from scratch is very time-consuming, and building an antenna is not the primary intent of our project. We conducted analysis on the antenna we acquired to measure its characteristics. The structure of the antenna consists of two metal electrodes with a dielectric layer sandwiched between them. We will build an L-band radiometer (1 - 2 GHz). Therefore, we want our antenna to resonate within that band. **Figure 3** shows the microstrip patch antenna we used. L and W represent the length and width of each patch, and h is the thickness of the dielectric material. For the antenna, we have $L=W= 6.85$ cm, and $h = 0.2$ cm.

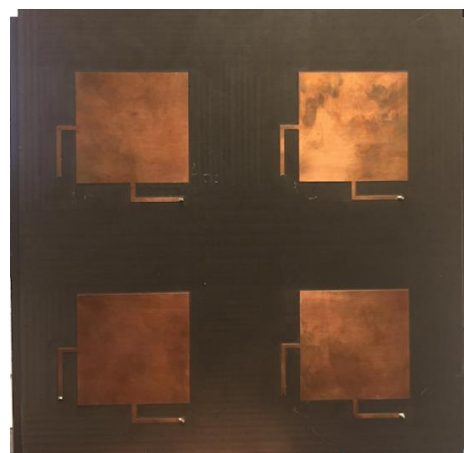


Figure 3. 2x2 Microstrip Patch Antenna

The equation for the resonant frequency of the patch antenna is:

$$f_0 = \frac{c}{2L\sqrt{\epsilon_r}}$$

where c is the speed of light, L is the patch length, and ϵ_r is the relative permittivity of the dielectric, $\epsilon_r = 2.406$.

To determine the different antenna parameters, we measured them using an HP Agilent network analyzer in the MIL lab to look at S_{11} . **Figure 4** shows the S_{11} parameters when the four patches are connected to the network analyzer. The first minimum point shows the measured resonant frequency to be $f = 1.412$ GHz with a BW= 20 MHz. Since the antenna has a resonant frequency of 1.412 GHz, it falls within the Radio Astronomy Band: 1.4-1.427 GHz. This means that we do not have to worry about Radio Frequency Interference (RFI) with cell phones and other devices with our antenna.

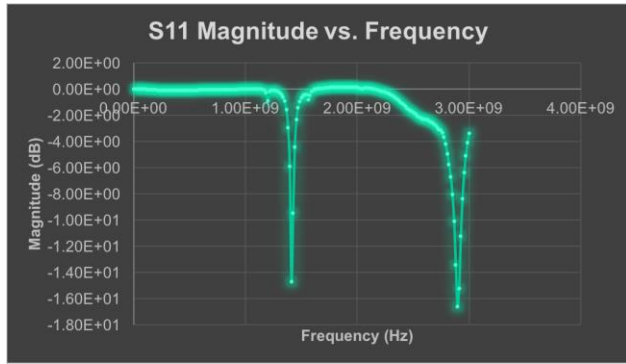


Figure 4. S_{11} vs. frequency showing 1.412 GHz as the resonant frequency

The reason why we see a second minimum point at almost double the initial frequency is because this is a multi-band antenna, meaning that it can resonate at different frequencies for different applications. However, since we are working in L-band, we are only interested in the first one and the second one will be filtered out using a bandpass system in the receiver circuit.

The receiver circuit consists of a cascade of a low-noise amplifier (LNA), bandpass filter, and a power amplifier (PA). We know that the ambient noise floor, tested a matched load, is about -75 dBm at room temperature. We know that we want our signal to be well above the noise floor, so we estimated that a ballpark of 40-50 dB of gain would be adequate. We received amplifiers and a bandpass filter from the MIRSL lab to test out the functionality and gain an understanding of the radiometer circuit. The bandpass filter is paired with the antenna; it has the same bandwidth and center frequency. When we connect the LNA to the bandpass filter to the PA and view the output on the spectrum analyzer, we see the shape of the filter’s frequency response. This is illustrated in **Figure 5**.

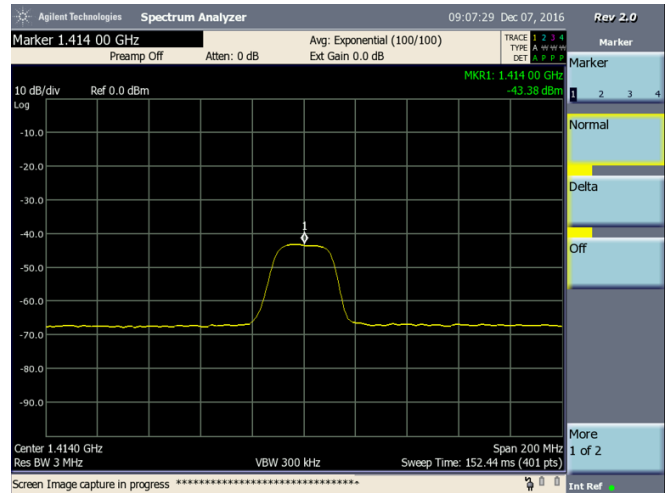


Figure 5. BPF frequency response on spectrum analyzer

One of the most crucial components in our receiver circuit is the power detector. Based on our readings from the spectrum analyzer and the power meter in the Microwaves Instructional Lab, we determined that the output of the LNA-BPF-PA cascaded had about -35 dBm of power. We wanted our power detector to be sensitive to the 20 MHz band that we are working in but not to the noise floor. The power detectors that we found produce a lower DC output voltage as their input power increases. The region where the power detector works best is where the plot of P_{in} vs. V_{out} is linear. To ensure that our detector will be sensitive only to frequencies in our range, we purchased one whose linear region begins at -45 dBm, below our signal level but comfortably above the noise floor. We decided to purchase the ZX47-55-S+. The plot of the detector’s output voltage vs input power, provided in its datasheet [9] is shown in **Figure 6**.

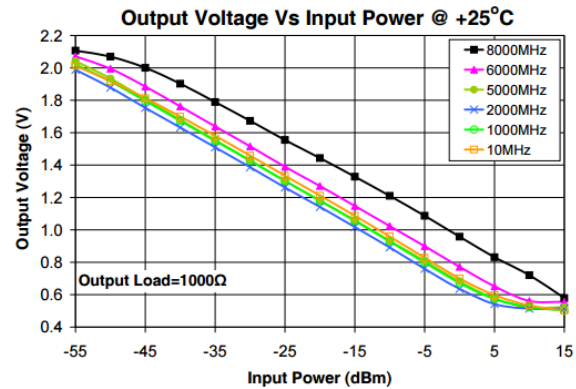


Figure 6. Power Detector Output Plot

The output of the power detector is noisy; we measured about 500mV of peak-to-peak noise on an oscilloscope. To eliminate this issue, we attach an RLC lowpass filter to the output before sampling it. The cutoff frequency f_c of the filter is about 16Hz. Plots of the filtered and

unfiltered output are compared in **Figure 7a** and **Figure 7b**, respectively.

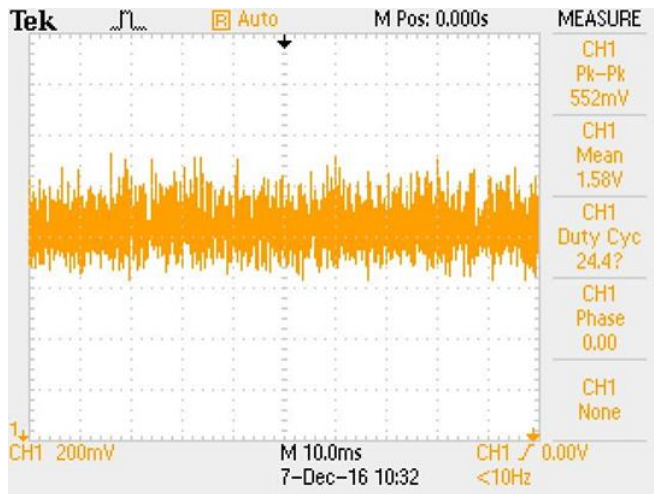


Figure 7a. Unfiltered Detector Output



Figure 7b. Filtered Detector Output

2. Control circuit

To calibrate our system properly, we need receiver output readings and temperature readings of our reference sources for each sample. The GPS receiver has a data rate of 10Hz, which sets the upper limit for the data rate of the rest of our system. We count a “supersample” as a receiver output reading from the antenna and each reference source and, the temperatures of the reference sources, which is five analog readings in total. Each of these supersamples will be stamped with a location and time from the GPS receiver. The microcontroller will also have to change the switch control logic using its GPIO pins in between receiver samples. Since all of this will only be happening around 10 Hz, this is not a hard requirement to meet.

The control circuit will determine if the switch outputs the antenna or the reference sources, it will sample the outputs from each sensor, and record all data to the SD

card. Initially we wanted to take supersamples at 10Hz, once every 100ms, but the settling time of the low pass filter is only 62.5ms. Since each source (antenna, noise diode, matched load) must be sampled within a supersample, and we cannot sample faster than the filter’s settling time, the slowest data rate for supersamples would be $3 \times 62.5\text{ms} = 187.5\text{ms}$. We decided to go with an even number and sample a source every 65ms, giving a supersample time of 195 ms.

We chose the Arduino Mega 2560 [10] to function as our control circuit. The Arduino comes with 54 I/O pins and 16 analog inputs, which will be used to coordinate switching and sample the sensor outputs. Another advantage of the Arduino Mega 2560 is that there are various breakout boards that can easily be incorporated with it. We purchased a GPS breakout board and an SD breakout board which both can be simply connected to the Arduino. The Arduino software is easy to learn how to use and program our own code. With a 16MHz processor, it has the ability to take the samples and coordinate the messages laid out in the previous paragraph.

The analog to digital converter (ADC) can limit our radiometric sensitivity, so its resolution must not put the sensitivity below 5K. To find the limit set by the ADC, simply find the change in power corresponding to an increase of one-bit level at the detector output, and convert this to a brightness temperature with the $P=KTB$ relation. We found that with the stock 10-bit ADC included with our Arduino, our sensitivity was 6.4K. To improve this, a 15-bit ADC breakout board was purchased. This changed the radiometric sensitivity limit set by the ADC to 0.38K.

3. Data Processing

To conserve computing power and make the design simpler, we will do all of our data processing after collection on a PC. A program will be required to read the data on the SD card line by line and run an algorithm to calculate the brightness temperatures that we need.

To understand our data, we need to create a lookup table of detector output voltage vs. input power. **Figure 4**, the plot provided in the datasheet, provides a rough idea of these values. However, more accurate numbers will be required to make calculations. A lookup table will be developed using technology in the MIL lab. A signal generator will be used to increase the input power to the detector in small increments, while a multimeter will record the output voltage. The data will be stored in an excel file and used later by the processing algorithm.

Our reference sources, a matched load and a noise source, are critical components. The program will first convert the recorded receiver output voltage to an input power, based on values from the lookup table. Resistive temperature detectors (RTD), which are devices whose resistance changes based on their temperature, will be used to find the temperature of each reference source. Since we will not be working in extreme temperatures, mostly any

RTD with a large dynamic range will suffice. The matched load produces the same noise power as is expected, $P = KTB$. The noise source, however, has a high Equivalent Noise Ratio (ENR). This means that it produces noise that is equal to the product of KTB and its ENR; it will radiate power as though it was much hotter than its actual temperature. We will multiply the measured temperature of the noise source by the ENR to find what temperature it appears to be, radiometrically. Since power has a linear relationship to temperature, our values of temperature and detector input power combined form a line on a temperature vs. power plot. By finding the point on this line where the measured antenna output power lies, the antenna temperature can be extrapolated. This calibration process will be carried out for every supersample.

The antenna temperature data will be combined with the GPS location data and used to create the moisture map in MATLAB. The location data will be used to generate a matrix, and each point in the matrix will be assigned a brightness temperature. The matrix will be plotted on a 2D graph, where different colors will represent different brightness temperatures. A plot for a sample 100x100 matrix with arbitrary values is provided in **Figure 8**.

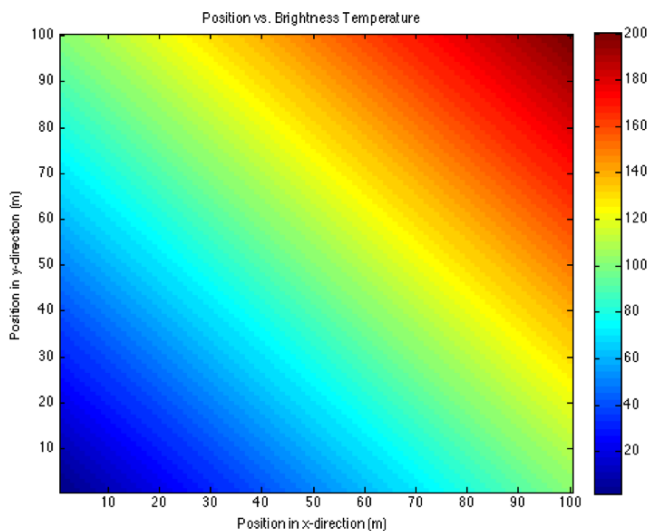


Figure 8. Arbitrary thermal map created on Matlab.

4. Power Supply

This project contains multiple parts which all incorporate active components. These components have either 5V or 15V supply voltages. In order to supply each of these devices with their desired voltages, we will be designing a Printed Circuit Board (PCB). This board will take in a master supply voltage and utilize buck and boost converters to provide the desired inputs. We chose to use the Turnigy 2.2 Lithium Ion battery for the master supply. This battery is capable of providing 11.6V. We know that our LNA requires a 15V supply voltage so we will need to use a boost converter to get that 11.6V to 15V. We will also need to incorporate a buck converter to get the 11.6V supply

down to a 5V supply. These components are readily accessible in a wide variety on websites like DigiKey and Mouser.

We chose to use this battery after we did some power measurements of the components we have been using in lab. We measured the current being drawn from our 5V and 15V supply, and then calculated the power from each supply. This Data can be seen in **Figure 9**.

Power Delivered by 5V source	Power Delivered by 15V source	Total Power Consumption
1.45 W	1.29 W	2.74 W

Figure 9. Measured Power Consumption

We then took into consideration the rest of the components that we were still looking to purchase to include in our calculation. With the new values we needed to equate them to an equivalent 11.1V current. When calculating this theoretical equivalent current with the values we incorporated we also included an efficiency factor of 70% to provide a conservative value. These new calculations can be seen in **Figure 10**. As you can see in these tables we will have a total power consumption of 4.22W. The Turnigy 2.2 battery offers 2.2Ah so based off of this fact we know that this circuitry can run for an approximated 6.04 hours. This means that our operation time will rely mainly on the drone’s operational time rather than the circuits operation time (If the drone path is permitted by our time restriction). On average an unloaded drone will fly for 45 minutes. With this being said, we hope to make the drone airborne for a 20-minute flight with the 3Kg receiver onboard.

Expected 5V consumption	Expected 15V consumption	Total expected consumption	Expected operation time
1.544 W	1.41 W	2.954 W	6.04 Hours

Figure 10. Anticipated Power Consumption

5. Noise Source

The ideal noise source for our project is the Pasternack PE8500. It has an ENR of 30dB, which gives us flexibility because a properly selected attenuator can bring this down to a lower level if the project requires it. It also has SMA connectors, a 50Ω impedance, and has an operating frequency range of 1GHz - 2GHz. The only challenge associated with utilizing the source in our project is that it requires a 28V supply, and thus a third DC-DC conversion circuit would be necessary. The PE8500 costs \$1,307.20, so a cheaper option must be used instead.

A cheaper option is the Noisecom NC302 noise diode. It is easily configured with the 15V supply, and Noisecom generously gave us three free samples of the NC302. We are having difficulties feeding the signal from the pins of the NC302 to our SMA connected system, which is a disadvantage compared to the PE8500, but to stay within budget and avoid designing a third DC-DC converter, we use the NC302.

III. PROJECT MANAGEMENT

Through consistent communication and collaboration our team has worked as a cohesive group since the beginning of this project. We communicate using a group text message to schedule weekly meetings and set times to work together on the project. We meet weekly with Professor Frasier to update him on the project status and ask any questions that may arise. The subsystems of our project are related and intertwined, so it is important that every member of our team have an understanding of each aspect of our system. Our team has done a great job at planning and using each other to solve any problems. In order to ensure we would meet our MDR deliverables we delegated specific tasks to each member of the group. Nick and Kyle focused on the receiver circuit including the radio frequency amplifying, filtering, and converting the RF signal into a DC voltage. We designated two people for this task because we felt the receiver circuit was a major aspect of our project. Erik focused on the control logic of our system including the microcontroller interaction with the switch and the data storage device. Mohamed focused on understanding the antenna that was generously given to our group by Professor Frasier. He also started working with Matlab to generate a grid of soil moisture vs. location.

MDR Deliverables	Status
RF circuit prototype	Completed
Detect changes in brightness temperature	Attempted, more definitive proof needed
Store data in SD card	Completed

Figure 11. MDR Deliverables

Since MDR, we have encased our project, purchased a 4-way power combiner, and have been able to collect data since we are no longer bound by the length of an extension cord. At FPR, our GPS receiver was not working well as we wanted it to, and therefore the data we presented was not fully convincing. In the week between FPR and demo day, we increased the precision of the data provided by the GPS receiver and then worked hard to collect as much

brightness temperature data as possible. Without this improvement in precision of the GPS data, our current thermal maps would not be convincing enough to demonstrate the project’s functionality.

IV. RESULTS

The final system specifications are compared to our initial goals in **Figure 12**.

Spec	Goal	Actual
Weight	< 5kg	3.63 kg
Radiometric Sensitivity	< 5 K	0.81 K
Operation time	> 30 minutes	2 Hours
Cost	<\$500	\$714.72

Figure 12. Final system specifications

Because of the new 15-bit ADC that we added, the sensitivity was limited by the noise figure of the receiver circuit. Using the following equation:

$$\Delta T_N = \frac{T_B + T_R}{\sqrt{B\tau}}$$

we found our radiometric sensitivity to be 1.4 K. T_B is the brightness temperature measured by the antenna, T_R is the noise temperature of the receiver, B is the system bandwidth, and τ is the integration time. Since we are measuring ambient noise, 300 K is a good estimate for T_B . With the gains and noise figures of the feed cables, the power combiner, the switch, the bandpass filter, and the amplifiers, the total system noise figure can be found with following equation:

$$F_{cas} = F_1 + \frac{F_2 - 1}{G_1} + \frac{F_3 - 1}{G_1 G_2} + \dots$$

This equation yields a system noise figure of 5.4dB, or 3.5 in linear units. T_R , the system noise temperature, can be found from the system noise figure, using the following equation:

$$T_R = 290K * (F_{cas} - 1)$$

This gives a system noise temperature value of 1308 K. Our system bandwidth, as previously mentioned, is 20 MHz, and our integration time is 65ms, our switching speed. Inserting these values into the equation for radiometric sensitivity gives a value of 1.41 K. To improve

this number even further, we used a 3 sample moving average on the power values from each source in watts, which increased the integration time to 195 ms. This change brought the sensitivity to 0.81 K.

To test how our system would detect differences in measured brightness temperature between soils of different moistures, we suspended the system in one location over wet and dry soil for two minutes each. **Figure 13** shows measured temperature of the dry spot vs. time, and **Figure 14** shows the same for wet soil. The measured mean brightness temperature was 243.5K for the dry soil, and 228.9K for the wet soil.

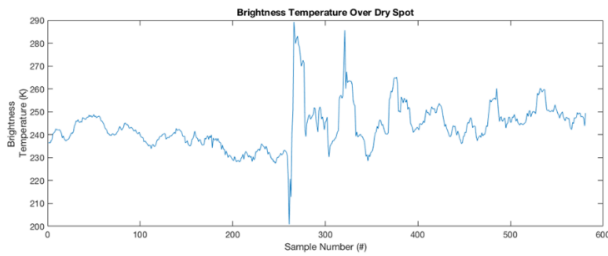


Figure 13. Brightness temperature over a dry spot

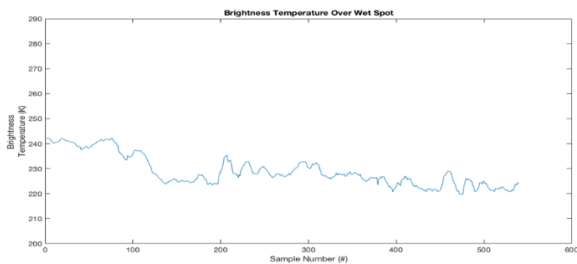


Figure 14. Brightness temperature over a wet spot

This data was saved on a micro SD card along with GPS coordinates and the ambient temperature. The difference we measured in brightness temperature shows that our system is capable of detecting changes in the power that is being radiated. The saved data was then processed on matlab to produce a map of brightness temperature over a given area. The path we walked can be seen as a scatterplot in **Figure 15**. This scatterplot is then interpolated to produce the thermal map that can be seen in **Figure 16**.

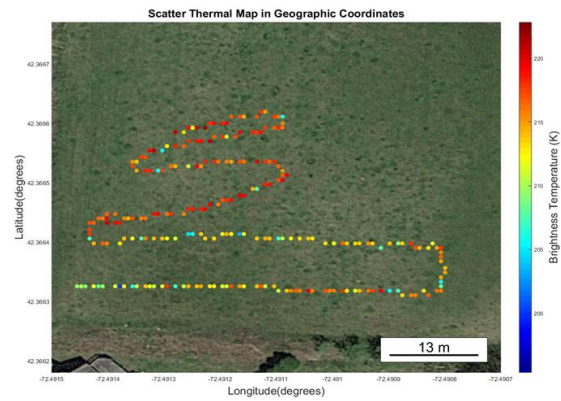


Figure 15. Scatter plot of brightness temperature of a farm in South Amherst

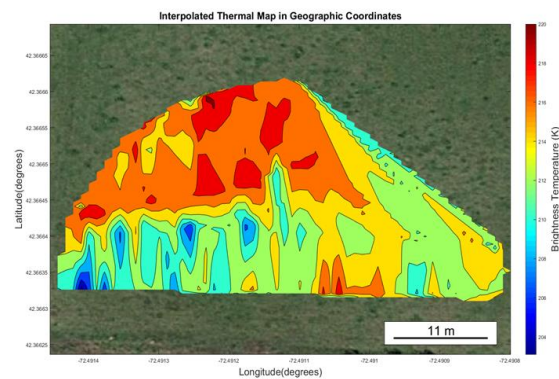


Figure 16. Interpolated plot of scatter data

Our system was contained inside a wooden box with a plexiglass cover. This cover allowed the GPS unit to receive a satellite fix while protecting the inner RF components as shown in **Figure 17**. The dimensions were measured to be an exact match to the size of the antenna allowing it to be mounted on the bottom of the box as can be seen in **Figure 3**.

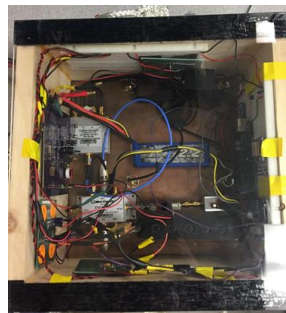


Figure 17. Full System encasing

The antenna seen in **Figure 3** was simulated in HFSS software to find its radiation pattern. The half power beam width was found to be 60°. Using this value, we calculated the area covered by the antenna in its far field to be roughly 104 sq ft. This was calculated using the fact that

our antenna would need to be 10 ft in the air to be in the far field region. The radiation pattern can be seen in **Figure 18**.

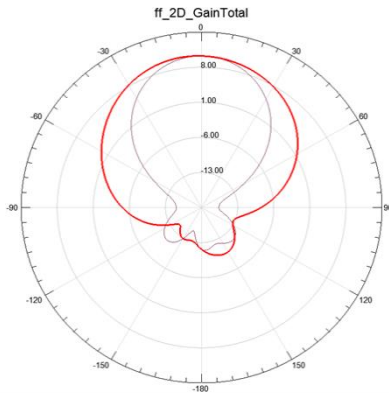


Figure 18. Antenna Radiation Pattern with 60° half-power beamwidth

Once the radiometer and housing were completed, we conducted a full analysis on the cost of our design, as well as a production cost if there were to be more than 1,000 of these units made. A tabulated cost of our final project design can be seen in **Figure 19**.

Part	Development	Production
PCB	\$28.67	\$22.34
Antenna	\$0	\$67.99
Low-Noise Amplifier	\$129.95	\$102.95
Power Amplifier	\$105.95	\$102.95
Band Pass Filter	\$39.95	\$38.45
Power Detector	\$89.95	\$70.45
Power Combiner	\$102.95	\$89.95
Arduino Microcontroller	\$37.95	\$32.65
GPS Receiver	\$39.95	\$31.96
15-bit ADC	\$14.95	\$11.96
Noise Diode	\$0	\$3
RF Switch	\$116.95	\$106.95
MicroSD Breakout	\$7.50	\$6.00
Total	\$714.72	\$687.60

Figure 19. Development and production cost of our system

The device was tested thoroughly in the Engineering Quad here on the UMass campus. The data we collected, however, contained a lot of RF interference. This noise that we were picking up was due to our close proximity to Marcus Hall and Knowles Engineering building, both of which contain microwaves labs. The data we collected in the Quad can be seen in **Figure 20**. Looking at this plot, there is a power spike up to roughly -22dB

among what appears to be large amounts of noise. A power spike that large is indicative of RF interference.

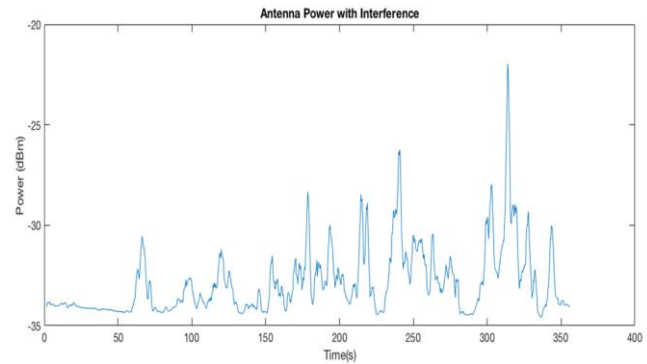


Figure 20. Antenna Power showing spiky jumps due to RFI in the Quad

To get accurate data, our team took the ESMS device to a large field in South Amherst, where a local farmer was kind enough to let us test our system in. The data we collected, which can be seen in **Figure 21**, clearly shows that there is no more RF interference.

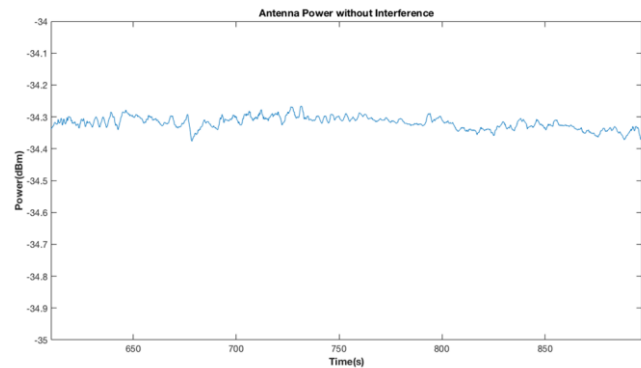


Figure 21. Stable antenna power readings in a farm

V. CONCLUSION

Overall, ESMS demonstrated that small scale radiometry for measuring soil moisture is possible. The project does not always get 100% accurate readings of brightness temperature, but it does read relative changes in moisture over an area. To improve its functionality, ESMS would ideally be fully consolidated on a microwave PCB. This would make it less susceptible to changes in gain due to movement, since there would be no coaxial connections. Additionally, it would improve the stability of the noise source, and therefore improve the effectiveness of gain calibration. It would also substantially reduce the size and weight of the project, and at that point a drone could potentially be used to deploy the system. This would allow for systematic, automated sweeping of an area; the only human effort required would be collecting the SD card from the system after deployment and running the file through the processing program. The development cost would increase,

but after completion the system would be easier to mass-produce.

VI. ACKNOWLEDGEMENTS

We would like to give a special thanks to our advisor, professor Frasier, for lending us his continuous guidance as well as providing inspiration for the project. We would also like to thank Professors Vouvakis and Anderson for their helpful and constructive criticism that led to system improvements. Also, we want to thank Professor Hollot for guiding us in the right direction throughout the year. Finally, a special thanks to NoiseComm for donating parts to our project.

VII. REFERENCES

- [1] Schmutz, T. "Remote Sensing of Soil Moisture with Microwave Radiometers." Transactions of the ASAE 26.3 (1983): 0748-753
- [2] Acevo-Herrera, Rene, Albert Aguasca, Xavier Bosch-Lluis, Adriano Camps, José Martínez-Fernández, Nilda Sánchez-Martín, and Carlos Pérez-Gutiérrez. "Design and First Results of an UAV-Borne L-Band Radiometer for Multiple Monitoring Purposes." Remote Sensing 2.7 (2010): 1662-679
- [3] Pozar, David M. "Microwave Engineering Education: From Field Theory to Circuit Theory." 2012 IEEE/MTT-S International Microwave Symposium Digest (2012): n. pag
- [4] Bevelacqua, Pete. "Microstrip (Patch) Antennas." Microstrip Antennas: The Patch Antenna. N.p., n.d. Web
- [5] Koivu, S. "Unknown Signal Detection Using a Digital Total-Power Radiometer with Finite Internal Precision." 2006 IEEE Instrumentation and Measurement Technology Conference Proceedings (2006): n. pag
- [6] "Brightness Temperature in Monitoring of Soil Wetness." SpringerReference (n.d.): n. pag
- [7] "Microstrip Antenna Array." Microstrip Patch Antennas (2010): 487-515
- [8] Farming: Wasteful Water Use." WWF. WWF Global, n.d. Web
- [9] Mini-Circuits, "Power Detector: -55dBm to +10dBm," ZX47-55 datasheet, Rev. D
- [10] Atmel, "8-bit Atmel Microcontroller with 16/32/64KB In-System Programmable Flash" Feb, 2014
- [11] Pozar, David M. Microwave engineering. 4th ed. Hoboken, NJ: Wiley, 2012. Print.